

# Crossed Beam Reactions of the Phenyl ( $C_6H_5$ ; $X^2A_1$ ) and Phenyl- $d_5$ Radical ( $C_6D_5$ ; $X^2A_1$ ) with 1,2-Butadiene ( $H_2CCCHCH_3$ ; $X^1A'$ )

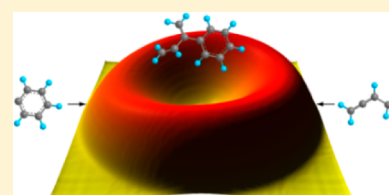
Tao Yang, Dorian S. N. Parker, Beni B. Dangi, and Ralf I. Kaiser\*

Department of Chemistry, University of Hawaii at Manoa, Honolulu, Hawaii 96822, United States

Vadim V. Kislov and Alexander M. Mebel

Department of Chemistry and Biochemistry, Florida International University, Miami, Florida 33174, United States

**ABSTRACT:** We explored the reactions on the phenyl ( $C_6H_5$ ;  $X^2A_1$ ) and phenyl- $d_5$  ( $C_6D_5$ ;  $X^2A_1$ ) radical with 1,2-butadiene ( $C_4H_6$ ;  $X^1A'$ ) at a collision energy of about  $52 \pm 3$  kJ mol $^{-1}$  in a crossed molecular beam apparatus. The reaction of phenyl with 1,2-butadiene is initiated by adding the phenyl radical with its radical center to the  $\pi$  electron density at the C1/C3 carbon atom of 1,2-butadiene. Later, the initial collision complexes isomerize via phenyl group migration from the C1/C3 carbon atoms to the C2 carbon atom of the allene moiety of 1,2-butadiene. The resulting intermediate undergoes unimolecular decomposition through hydrogen atom emission from the methyl group of the 1,2-butadiene moiety via a rather loose exit transition state leading to 2-phenyl-1,3-butadiene in an overall exoergic reaction ( $\Delta_R G = -72 \pm 10$  kJ mol $^{-1}$ ). This finding reveals the strong collision-energy dependence of this system when the data are compared with those of the phenyl radical with 1,2-butadiene previously recorded at collision energies up to 160 kJ mol $^{-1}$ , with the previous study exhibiting the thermodynamically less stable 1-phenyl-3-methylallene ( $\Delta_R G = -33 \pm 10$  kJ mol $^{-1}$ ) and 1-phenyl-2-butyne ( $\Delta_R G = -24 \pm 10$  kJ mol $^{-1}$ ) to be the dominant products.



## 1. INTRODUCTION

The increasing interests in the past decades in polycyclic aromatic hydrocarbons (PAHs) and soot particles have been attributed to their important roles in combustion processes and terrestrial and extraterrestrial environments.<sup>1–5</sup> Largely produced in the combustion of carbonaceous materials such as fossil fuels, coals, and biomasses, they are considered as severe air and marine pollutants,<sup>4,6,7</sup> further contributing to global warming.<sup>8</sup> Generated as toxic byproducts in the incomplete combustion processes, PAHs such as benzo[*a*]pyrene have been identified as carcinogenic<sup>9,10</sup> and mutagenic.<sup>11</sup> In extraterrestrial environments, PAHs are also discovered ubiquitously in the interstellar medium (ISM),<sup>5</sup> in hydrocarbon rich atmospheres of the planets and their moons such as in Titan's atmosphere,<sup>12</sup> and in carbonaceous chondrite meteorites such as the Murchison chondrite,<sup>13</sup> which can thus provide a detailed record to the chemical evolutions prior to the origin of life.

However, the formation mechanisms of PAHs have not been completely understood. It is strongly believed that the phenyl radical ( $C_6H_5$ ) plays an important role in the stepwise molecular growth pathways to the formation of PAHs.<sup>1,14</sup> Bicyclic PAHs such as naphthalene ( $C_{10}H_8$ ) are suggested to be formed either by the hydrogen abstraction–acetylene addition (HACA) mechanism<sup>14–16</sup> or through the phenyl addition–cyclization (PAC) reactions with unsaturated hydrocarbons such as alkynes,<sup>17</sup> olefins,<sup>18,19</sup> and aromatic molecules.<sup>20</sup> Parker et al. provided an alternative pathway to naphthalene synthesis ( $C_{10}H_8$ ), in which the phenyl radical reacts via a submerged barrier with vinylacetylene ( $C_4H_4$ ).<sup>21</sup> In addition, indene ( $C_9H_8$ )

can be formed via bimolecular reactions of phenyl radicals with two  $C_3H_4$  isomers: allene ( $H_2CCCH_2$ ) and methylacetylene ( $CH_3CCH$ ).<sup>22</sup>

Specifically, in recent years extensive experimental investigations<sup>23–27</sup> have been performed on the reactions of phenyl radicals with distinct  $C_4H_6$  isomers. In a chemical reactor of 300 Torr and 873 K, the reaction of phenyl with 1,3-butadiene was conducted and the photoionization efficiency (PIE) curves were recorded by interrogating and photoionizing the product isomers with aid of the tunable ultraviolet (VUV) light from the Advanced Light Source.<sup>27</sup> The product distributions were then obtained by fitting in a linear combination of PIE curves for individual  $C_{10}H_{10}$ ,  $C_9H_8$ , and  $C_8H_8$  isomers. Combined with electronic structure calculations, the authors identified that 1,4-dihydronaphthalene ( $C_{10}H_{10}$ ), 1-phenyl-1,3-butadiene ( $C_{10}H_{10}$ ), and styrene ( $C_8H_8$ ) were formed under combustion-like conditions, with 1,4-dihydronaphthalene (major product) and 1-phenyl-1,3-butadiene (minor product) also identified in crossed molecular beam studies (Figure 1).<sup>26</sup> However, the data from the pyrolytic reactor also suggested that 1-methylindene ( $C_{10}H_{10}$ ), indene ( $C_9H_8$ ), phenylallene ( $C_9H_8$ ), and 1-phenyl-1-methylacetylene ( $C_9H_8$ ) were synthesized; these products should not be formed via the reaction of phenyl with 1,3-butadiene under single collision conditions (Figure 1). The authors suggested that the isomerization of 1,3-butadiene in the chemical reactor, either by thermal

Received: November 27, 2013

Revised: May 20, 2014

Published: June 2, 2014

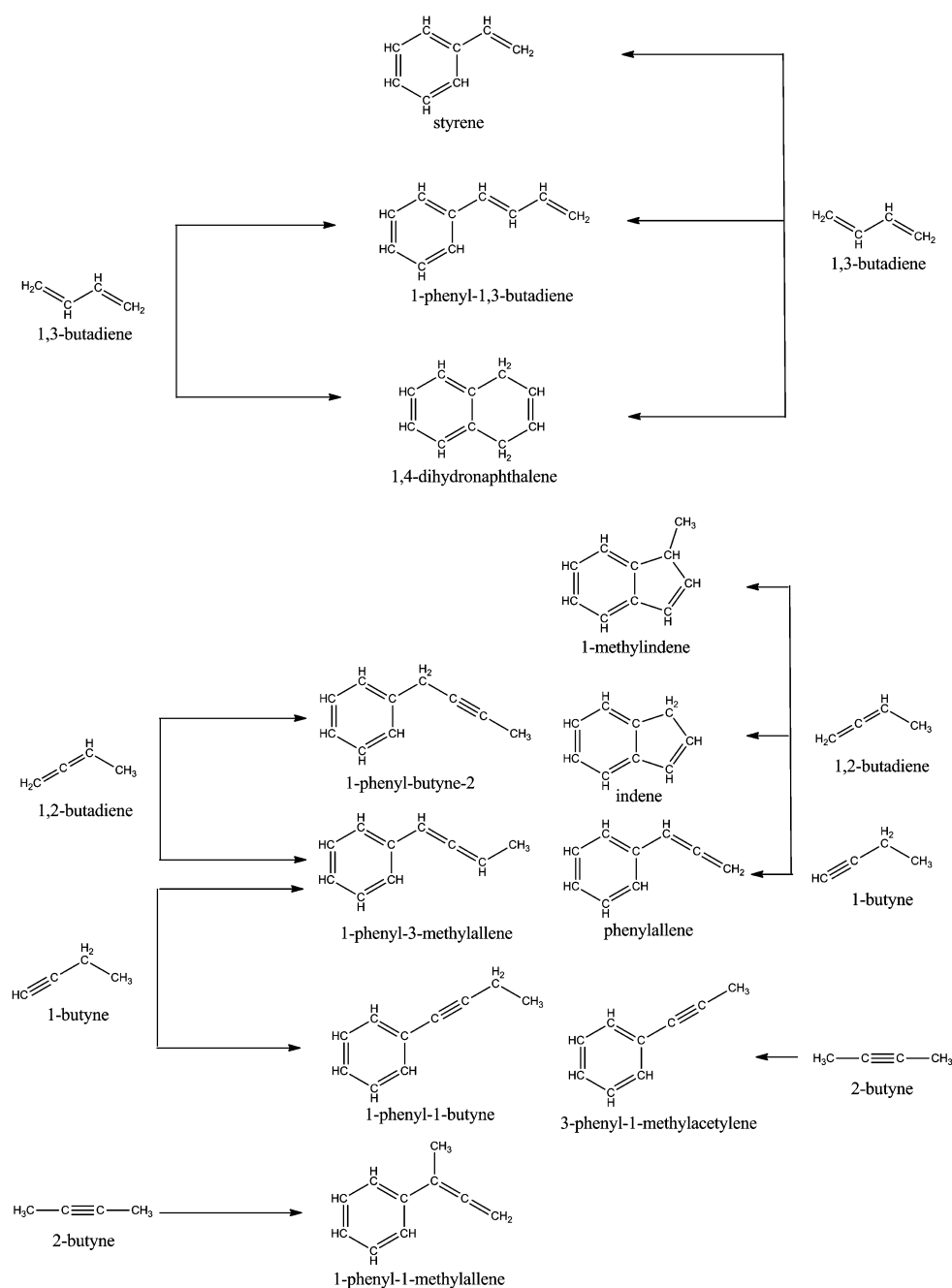


**Figure 1.** Reaction products of the phenyl radical with four  $C_4H_6$  isomers (1,3-butadiene, 1,2-butadiene, 1-butyne, 2-butyne) under single collision conditions obtained in a crossed molecular beam machine (left) and under combustion-like conditions within a chemical reactor (right).

means or by hydrogen atom assistance, resulted in the formation of three less stable  $C_4H_6$  isomers: 1,2-butadiene, 1-butyne, and 2-butyne. The addition of phenyl to the C1 carbon of 1,2-butadiene leads to the formation of 1-phenyl-2-buten-2-yl, which can generate indene and 1-methylindene via ring closure and hydrogen shifts followed by methyl and hydrogen losses, respectively. The addition of phenyl to the C3 carbon atom of 1,2-butadiene forms 3-phenyl-2-buten-2-yl, which then fragments to phenylallene via a methyl group loss.

Further, as probed in crossed molecular beam experiments, the reactions of phenyl with four  $C_4H_6$  isomers were conducted under single collision conditions at collision energies up to  $156 \text{ kJ mol}^{-1}$ : 1,3-butadiene ( $H_2CCHCHCH_2$ ),<sup>23</sup> 1,2-butadiene ( $H_2CCCHCH_3$ ),<sup>24</sup> 1-butyne ( $HCCC_2H_5$ ),<sup>25</sup> and 2-butyne

( $H_3CCCCH_3$ ).<sup>25</sup> As a consequence, 1-phenyl-1,3-butadiene (from 1,3-butadiene),<sup>23</sup> 1-phenyl-3-methylallene and 1-phenyl-butyne-2 (from 1,2-butadiene),<sup>24</sup> 1-phenyl-1-butyne and 1-phenyl-3-methylallene (from 1-butyne),<sup>25</sup> and 1-phenyl-1-methylallene (from 2-butyne)<sup>25</sup> were formed (Figure 1). In these systems, the lifetimes of the reaction intermediates were found to be too low to allow isomerization via hydrogen shifts with/without further ring closure processes and hence PAH formation. Later, our group exploited a photodissociation source to produce a supersonic beam of phenyl radicals with typical velocities down to only  $1600 \text{ ms}^{-1}$ , which make it possible to perform the crossed beam reactions at lower collision energies of about  $45 \text{ kJ mol}^{-1}$ .<sup>21,22,26,28</sup> For example, in the crossed beam reaction of phenyl with 1,3-butadiene, the major product

1,4-dihydronaphthalene was formed through the isomerization and ring closure processes of the  $C_{10}H_{11}$  collision complex (phenyl addition to C1/C4 carbon atom of 1,3-butadiene) with a hydrogen emission from the phenyl moiety at the bridging carbon, whereas the minor product 1-phenyl-1,3-butadiene was formed via a hydrogen ejection from the terminal  $CH_2$  group of the 1,3-butadiene moiety in the initial  $C_{10}H_{11}$  collision complex.<sup>26</sup> These considerations suggest that a change in the collision energy can dramatically alter the product spectrum and branching ratios with PAH-like species preferentially formed at lower collision energies. Here, we reinvestigate the reactions of the phenyl/phenyl- $d_5$  radical with 1,2-butadiene at low collision energies in a crossed molecular beam machine, thus probing to what extent bicyclic PAH-like species can be formed. Further, replacing phenyl by phenyl- $d_5$  will also shed some light if the hydrogen atom is emitted from the 1,2-butadiene reactant or from the phenyl radical (or both).

## 2. EXPERIMENTAL SETUP

The reactions of the phenyl radical ( $C_6H_5$ ;  $X^2A_1$ ) and of the phenyl- $d_5$  radical ( $C_6D_5$ ;  $X^2A_1$ ) with 1,2-butadiene ( $C_4H_6$ ;  $X^1A'$ ) were conducted in a crossed molecular beam apparatus at the University of Hawaii at Manoa.<sup>29–32</sup> Helium (99.9999%; Airgas Gaspro) of 1.8 atm was introduced into the stainless steel bubbler containing chlorobenzene ( $C_6H_5Cl$ ; 99.9%; Sigma-Aldrich)/chlorobenzene- $d_5$  ( $C_6D_5Cl$ ; 99 atom % D; Alfa Aesar), and the seeded chlorobenzene/chlorobenzene- $d_5$  beam was released into the primary chamber via a pulsed valve (Piezo Disk Translator; part number P-286.23; Physik Instrumente) at a repetition rate of 120 Hz. The seeded molecular beam was then photodissociated perpendicularly at a spot 1 mm downstream from the nozzle by a focused 193 nm laser beam from a Lambda Physik Compex 110 Excimer laser, at a repetition rate of 60 Hz and energy of  $12 \pm 2$  mJ. A portion of the radical beam is selected by a four-slot chopper wheel equipped after the skimmer, and intercepted perpendicularly the secondary molecular beam of 1,2-butadiene (98%; ChemSampCo) controlled by another pulsed valve at the repetition rate of 120 Hz. We optimized the delay times of the pulsed valves and the laser to obtain the best signal-to-noise ratios of the reactive scattering products. In our experiment, the photodiode equipped near the chopper wheel provided the time zero trigger; the primary and secondary pulsed valves were triggered at 1890 and 1850  $\mu s$ , respectively. The excimer laser was fired with a delay time of 162  $\mu s$  with respect to the primary pulsed valve (Table 1).

**Table 1. Primary and Secondary Beam Peak Velocities ( $v_p$ ), Speed Ratios ( $S$ ), Collision Energies ( $E_c$ ), and Center-of-Mass Angles ( $\Theta_{CM}$ ) for the Reactions of the Phenyl ( $C_6H_5$ ;  $X^2A_1$ ) and Phenyl- $d_5$  Radical ( $C_6H_5$ ;  $X^2A_1$ ) with 1,2-Butadiene ( $C_4H_6$ ;  $X^1A'$ )**

beam	$v_p$ ( $ms^{-1}$ )	$S$	$E_c$ ( $kJ\ mol^{-1}$ )	$\Theta_{CM}$
$C_6H_5(X^2A_1)$	$1634 \pm 15$	$9.8 \pm 0.8$	$52 \pm 3$	$18.6 \pm 0.5$
$C_6D_5(X^2A_1)$	$1631 \pm 15$	$14.5 \pm 0.9$	$53 \pm 3$	$17.6 \pm 0.5$
1,2- $C_4H_6(X^1A')$	$785 \pm 18$	$8.7 \pm 0.5$		

The reactive scattering products then entered the detection chamber in a three-stage differential pumping system. The electron impact ionized products (ionization energy of 80 eV with emission current of 2 mA) passed through the Extrel QC 150 quadrupole mass spectrometer with a desired mass-to-charge

( $m/z$ ) ratio and flew toward a stainless steel target coated with aluminum operating at  $-22.5$  kV. The impinging ions initiated a cascade of electrons, which were accelerated onto an aluminum-coated organic scintillator eventually initiating photons that were detected by a photomultiplier. The signal was further discriminated (1.6 mV) and fed into a multichannel scalar. We recorded up to  $3 \times 10^5$  TOF spectra for each angle, integrated and normalized the angular-resolved TOF spectra, and extracted the laboratory product angular distribution at the defined mass-to-charge ratio. We therefore utilized a forward-convolution routine<sup>33–35</sup> and a set of parametrized functions of the product translational energy distribution  $P(E_T)$  and angular distribution  $T(\theta)$  in the center-of-mass (CM) frame, to iteratively fit the experimental TOF spectra and the LAB angular distribution until the best fits were reached. This will also yield the product flux contour map  $I(\theta, u) = P(u) \times T(\theta)$ , which describes the “image” of the reaction.<sup>26</sup>

## 3. EXPERIMENTAL RESULTS

We recorded the reactive scattering signal at  $m/z$  of 130 ( $C_{10}H_{10}^+$ ) and 129 ( $C_{10}H_9^+$ ) for the reaction of phenyl with 1,2-butadiene. The TOF spectra at  $m/z = 130$  and 129 were superimposable after scaling, with higher intensities and better signal-to-noise ratios at  $m/z = 130$ . Because the scaled TOF spectra of  $m/z = 130$  and 129 were identical within our detection limit, the signal at  $m/z = 129$  originates from the further dissociation of the  $C_{10}H_{10}$  product in the electron impact ionizer. Thus, we recorded the TOF spectra at  $m/z = 130$  ( $C_{10}H_{10}^+$ ; Figure 2, left) and obtained the corresponding LAB angular distribution (Figure 3, left). Therefore, we can conclude that there exists at least one hydrogen emission channel for the reaction of phenyl with 1,2-butadiene. Note that signal at  $m/z = 131$  was also observed. This actually originated from  $^{13}CC_9H_{10}$ , and not from the adduct ( $C_{10}H_{11}$ ) because the intensity of signal at  $m/z = 131$  was about 10% of that at  $m/z = 130$ , and the TOF spectra at  $m/z = 131$  and 130 overlapped with each other after scaling as well. Because both the phenyl radical and 1,2-butadiene can lose a hydrogen atom, we also explored to what extent the hydrogen atom is emitted from the 1,2-butadiene reactant and/or from the phenyl radical. Therefore, we performed the reaction of phenyl- $d_5$  with 1,2-butadiene. We monitored reactive scattering signal at  $m/z = 135$  ( $C_{10}D_5H_5^+$ ) and  $m/z = 134$  ( $C_{10}D_5H_4^+/C_{10}D_4H_6^+$ ). Once again, we found that the TOF spectra were superimposable after scaling of data at  $m/z = 135$  and 134. Consequently, the signal at  $m/z = 134$  originates from the further dissociation of the  $C_{10}D_5H_5$  product in the electron impact ionizer. Further, we provided explicit evidence that atomic hydrogen is lost from 1,2-butadiene and that within the sensitivity of our system, no deuterium atom is emitted. Therefore, we collected TOF spectra at  $m/z = 135$  ( $C_{10}D_5H_5^+$ ; Figure 2, right) and obtained the corresponding LAB angular distribution (Figure 3, right). Note that by comparing the absolute intensities of the reactive scattering signal for the phenyl with 1,2-butadiene and the phenyl- $d_5$  with 1,2-butadiene systems, we find the reactive scattering signal for both systems range within a few percent after scaling with respect to the primary beam intensities. This provides further evidence that the hydrogen loss originates from the 1,2-butadiene molecule. The corresponding LAB angular distributions (Figure 3) of both systems span only about  $17^\circ$  in the scattering plane. Finally, we need to stress that we also attempted to search for the methyl loss channel as detected in the crossed beam reactions of phenyl/phenyl- $d_5$  with propene

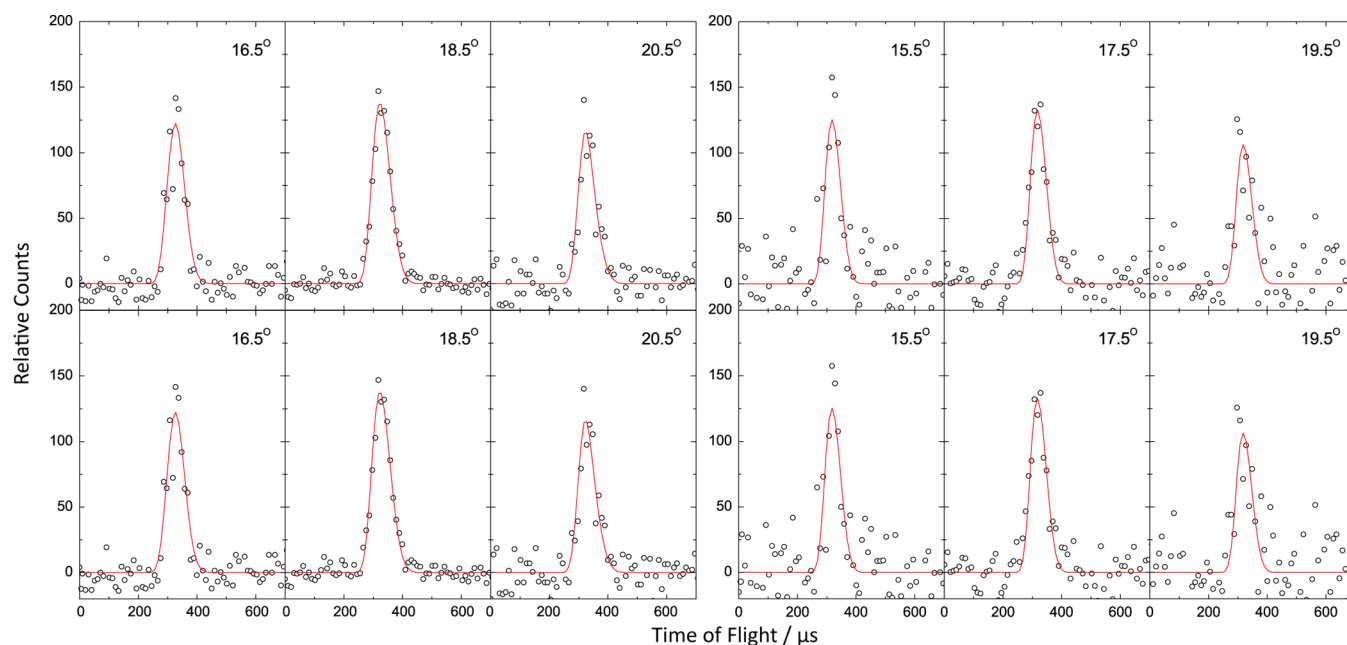


**Figure 2.** Selected time-of-flight (TOF) spectra at mass-to-charge ( $m/z$ ) ratios of 130 ( $C_{10}H_{10}^+$ , left) and 135 ( $C_{10}D_5H_5^+$ , right) for the reactions of the phenyl radical ( $C_6H_5$ ;  $X^2A_1$ ) and the phenyl- $d_5$  radical ( $C_6D_5$ ;  $X^2A_1$ ) with 1,2-butadiene ( $C_4H_6$ ;  $X^1A'$ ) at low reaction exoergicity of  $75 \text{ kJ mol}^{-1}$  (upper) and at high reaction exoergicity of  $158 \text{ kJ mol}^{-1}$  (lower), respectively. The circles represent the experimental data points, and the solid lines represent the fits using the forward-convolution routine.

( $CH_3CHCH_2$ )<sup>28</sup> and of boron monoxide radical (BO) with methylacetylene ( $CH_3CCH$ )<sup>36</sup> and with dimethylacetylene ( $CH_3CCCH_3$ ).<sup>37</sup> However, we could not detect any reactive scattering signal at  $m/z = 116$  and  $m/z = 121$  in the reactions of the phenyl/phenyl- $d_5$  radical with 1,2-butadiene, respectively. Therefore, we can conclude that the methyl loss pathway, at least within the detection limits of our system, is undetected.

Having identified that the hydrogen emission originates from the 1,2-butadiene molecule, we can now obtain more information on the underlying reaction dynamics by transferring the laboratory data into the CM reference frame (Figure 4). We emphasize that the fits exploited parametrized CM functions so that we can compare the results of the present experiments with those conducted previously in our laboratory at elevated collision energies of up to  $160 \text{ kJ mol}^{-1}$ . For the phenyl plus 1,2-butadiene and phenyl- $d_5$  plus 1,2-butadiene systems, the recorded TOF spectra and LAB angular distributions were fit with a single channel of a mass combination of 130 amu ( $C_{10}H_{10}$ ) plus 1 and 135 amu ( $C_{10}D_5H_5$ ) plus 1 amu (H), respectively. It should be noted that the fits were relatively insensitive to the high energy cutoff and the distribution maxima of the CM translational energy distributions ( $P(E_T)$ 's). Here, for both the phenyl/phenyl- $d_5$  with 1,2-butadiene reactions, best fits were obtained with  $P(E_T)$ 's that can be extended up to  $128 \pm 25 \text{ kJ mol}^{-1}$  (Figure 4, upper left) and even  $210 \pm 25 \text{ kJ mol}^{-1}$  (Figure 4, lower left). For the molecules formed without internal excitation, the high-energy cutoff represents the sum of the absolute reaction energy and the collision energy; therefore, we determined reaction energies between  $75 \pm 28$  and  $158 \pm 28 \text{ kJ mol}^{-1}$ . In addition, the  $P(E_T)$ 's depict distribution maxima between 25 and  $45 \text{ kJ mol}^{-1}$ . It is noteworthy that the energetics of the systems are not well constrained because fits of the TOF spectra (Figure 2) and LAB angular distributions (Figure 3) for both reaction systems can be obtained for essentially any reaction energy between  $75 \pm 28$  and  $158 \pm 28 \text{ kJ mol}^{-1}$ . We also attempted to fit the laboratory data with lower reaction

exoergicities down to  $33 \pm 10$  and  $24 \pm 10 \text{ kJ mol}^{-1}$ , i.e., the reaction energies associated with the formation of 1-phenyl-3-methylallene and 1-phenyl-butyne-2 as elucidated in our previous studies at collision energies as high as  $160 \text{ kJ mol}^{-1}$ .<sup>24</sup> However, the laboratory data could not be fit with such low reaction energies because the simulated laboratory angular distributions were, due to the low reaction exoergicity, much narrower than the experimental data (Figure 3). Therefore, we can conclude that the reaction exoergicities of the phenyl with 1,2-butadiene and phenyl- $d_5$  with 1,2-butadiene systems range between  $75 \pm 28$  and  $158 \pm 28 \text{ kJ mol}^{-1}$ .

We can also obtain additional information from the CM angular distributions  $T(\theta)$ 's. For the reactions of phenyl/phenyl- $d_5$  with 1,2-butadiene, both distributions for each respective reaction system are identical and depict intensities all over the complete angular range from  $0^\circ$  to  $180^\circ$  (Figure 4, right). This result indicates indirect reaction dynamics via the formation of bound  $C_{10}H_{11}/C_{10}D_5H_6$  intermediate(s).<sup>38</sup> Also, both distributions are slightly asymmetric around  $90^\circ$  and depict preferential fluxes in the forward hemispheres, with respect to the phenyl/phenyl- $d_5$  radical beam; this trend is also reflected in the flux contour map (Figure 5). The ratios of intensities at poles,  $I(180^\circ)/I(0^\circ)$ , are about 0.8 for both systems, which allows us to conclude that the lifetime(s) of the bound  $C_{10}H_{11}/C_{10}D_5H_6$  intermediate(s) is comparable to their rotational period(s).<sup>39</sup>

#### 4. THEORETICAL RESULTS

In the case of polyatomic systems, it is beneficial to combine the experimental data with the electronic structure and statistical calculations (Figures 6 and 7). These computations were conducted at the G3(MP2,CC)//B3LYP/6-311G\*\* level of theory<sup>40</sup> using the GAUSSIAN 98<sup>41</sup> and MOLPRO 2002<sup>42</sup> program packages yielding accuracies of the energies of the intermediates and products within  $\pm 10 \text{ kJ mol}^{-1}$ .<sup>43</sup> Further, Rice–Ramsperger–Kassel–Marcus (RRKM) calculations were carried out to compute the branching ratios of the products.<sup>43,44</sup>

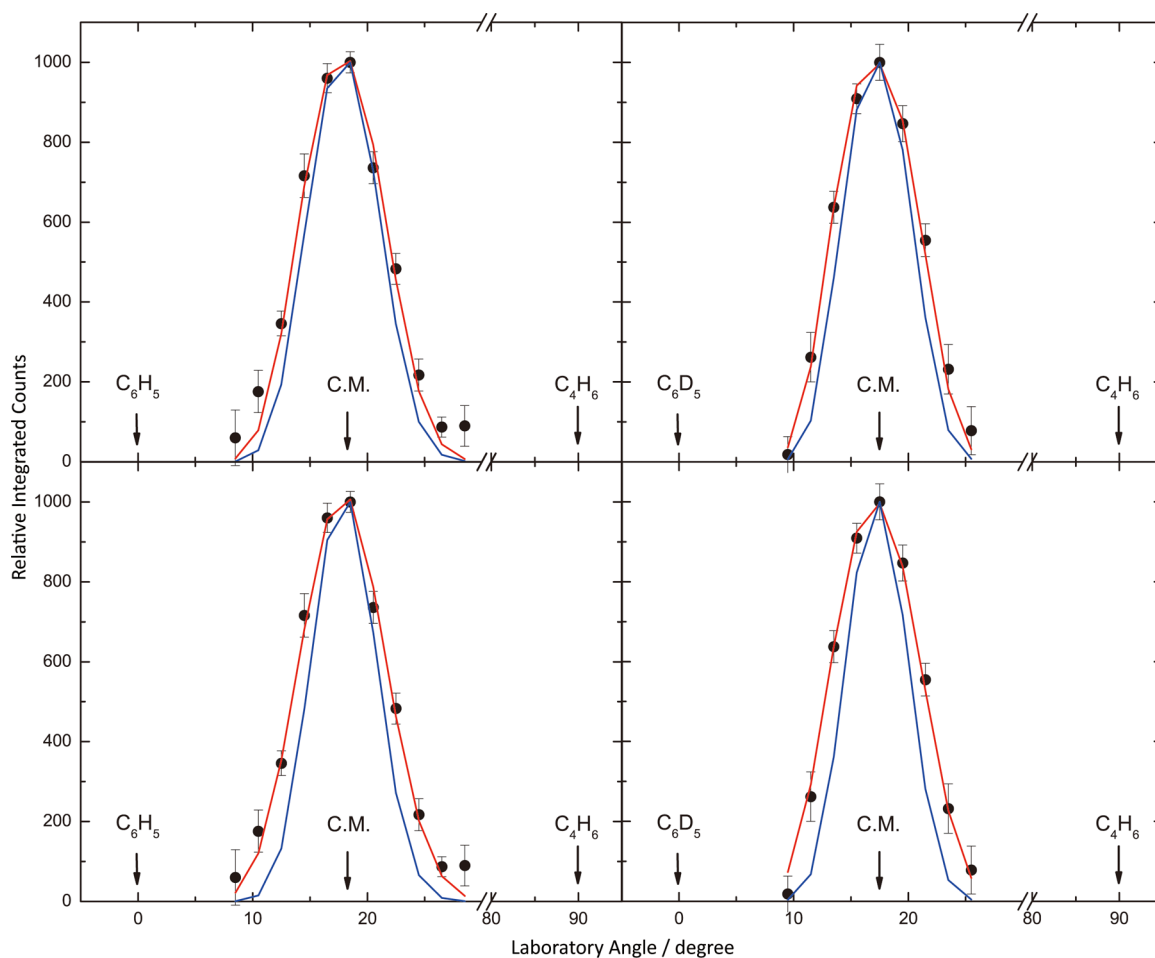


**Figure 3.** Laboratory (LAB) angular distributions of signal at  $m/z$  of 130 ( $C_{10}H_{10}^+$ , left) and 135 ( $C_{10}D_5H_5^+$ , right), for the reactions of the phenyl radical ( $C_6H_5$ ;  $X^2A_1$ ) and phenyl- $d_5$  radical ( $C_6D_5$ ;  $X^2A_1$ ) with 1,2-butadiene ( $C_4H_6$ ;  $X^1A'$ ) at low reaction exoergicity of  $75 \text{ kJ mol}^{-1}$  (upper) and at high reaction exoergicity of  $158 \text{ kJ mol}^{-1}$  (lower), respectively. The solid circles depict the experimental data and the red solid lines represent the calculated best fits. For comparison, the blue lines represent the calculated distribution assuming a reaction exoergicity of only  $30 \text{ kJ mol}^{-1}$ .

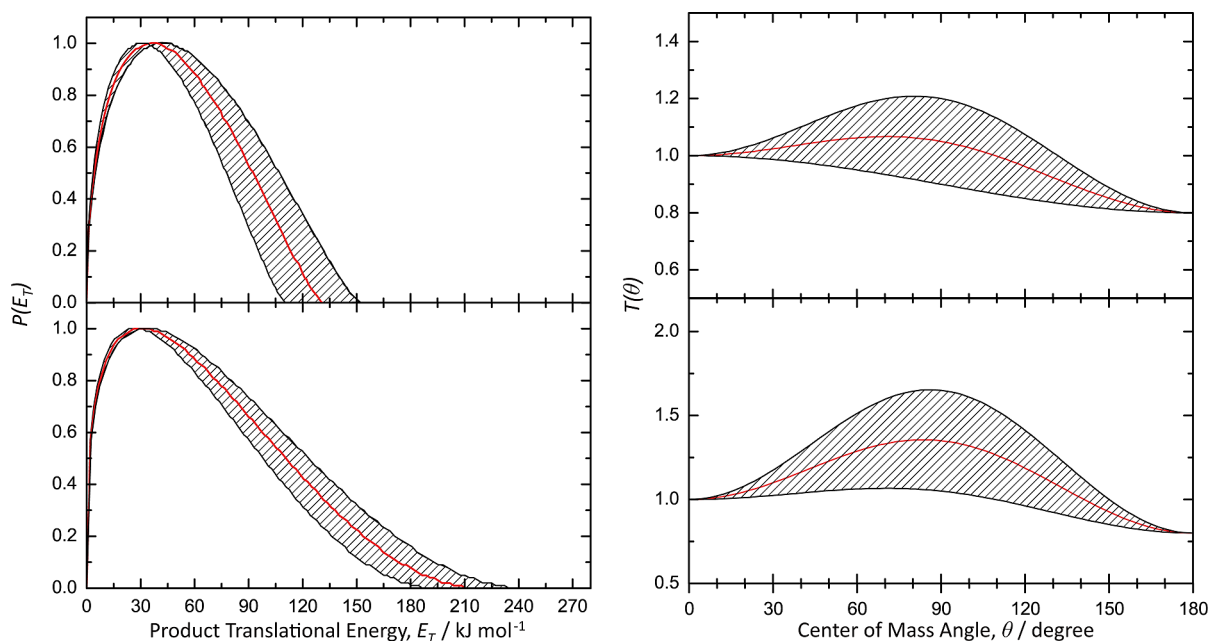


**Figure 4.** Center-of-mass translational energy distributions (left) and angular distributions (right) exploited to fit the laboratory data of the phenyl/phenyl- $d_5$  with 1,2-butadiene reactions via a single channel reaction leading to  $C_{10}H_{10}$  and  $C_{10}H_5D_5$  isomers via atomic hydrogen losses, at low reaction exoergicity of  $75 \text{ kJ mol}^{-1}$  (upper) and at high reaction exoergicity of  $158 \text{ kJ mol}^{-1}$  (lower), respectively. The hatched areas represent the experimental error limits.



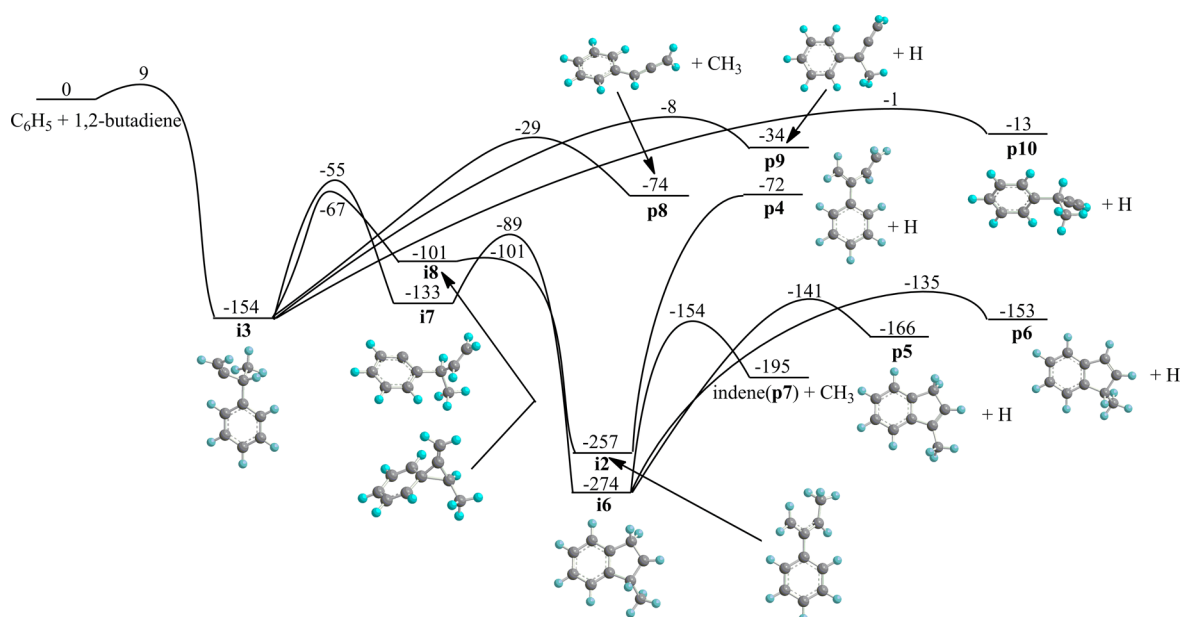


**Figure 7.** Potential energy surface for the reaction of the phenyl radical addition to the C3 carbon atom of 1,2-butadiene calculated at the G3(MP2,CC)//B3LYP/6-311G\*\* level of theory. All relative energies are given in  $\text{kJ mol}^{-1}$ .

a hydrogen migration from the C2 carbon atom of the phenyl group to the C2 carbon atom of the 1,2-butadiene moiety, yielding **i4**. Alternatively, **i1** can isomerize via ring closure to the bicyclic intermediate **i5**; considering the inherent barriers, the isomerization of **i1** to **i5** should be preferential. The latter is metastable and only has to overcome a barrier of  $3 \text{ kJ mol}^{-1}$  to yield **i2**, whereas **i4** can undergo a ring-closure process to yield **i6**. The intermediate **i6** then ejects a hydrogen atom yielding **p5** (3-methylindene) and/or **p6** (1-methylindene) or a methyl group to form **p7** (indene). Finally, we have to consider the isomerization pathways for **i3**. Similar to **i1**, **i3** can isomerize to **i2** by formal migration of the phenyl moiety over the carbon-carbon double bond via a metastable intermediate **i8**. Also, a hydrogen shift from the C2 carbon atom of the phenyl to the 1,2-butadiene moiety yields **i7**, which eventually isomerizes to **i6**. In summary, considering the inherent barriers to isomerization, the initial collision complexes **i1** (**i3**) either decompose to **p1** (**p9**), **p2** (**p10**), and/or **p3** (**p8**) or isomerize eventually to **i2** with the latter ejecting an atomic hydrogen to form **p4** (2-phenyl-1,3-butadiene). Although the methyl-substituted indenenes (**p5** and/or **p6**) and indene (**p7**) can be formed following isomerization of **i1** or **i3** to **i6**, their production is less feasible due to the higher barriers along the **i1** (**i3**)  $\rightarrow$  **i4** (**i7**)  $\rightarrow$  **i6** pathways as compared to those for **i1** (**i3**)  $\rightarrow$  **i5** (**i8**)  $\rightarrow$  **i2**. It should be also noted that besides the methyl loss channels **i1** (**i3**)  $\rightarrow$  **p3** (**p8**), the energetics of all other respective isomerization and dissociation pathways of **i1** and **i3** are rather similar and within  $10 \text{ kJ mol}^{-1}$ .

## 5. DISCUSSION

Now we combine the theoretical predictions with the experimental data and summarize the results as R1-R5.

(R1) The reactions of phenyl with 1,2-butadiene and phenyl- $d_5$  with 1,2-butadiene lead to the formation of  $\text{C}_{10}\text{H}_{10}$  and  $\text{C}_{10}\text{D}_5\text{H}_5$  isomers via atomic hydrogen losses, respectively.

(R2) No methyl loss channel was observed in the present experiments.

(R3) Detailed studies about phenyl- $d_5$  with 1,2-butadiene reaction system exhibit that the hydrogen is lost exclusively from the 1,2-butadiene reactant, but not from the phenyl radical.

(R4) The reactions follow indirect scattering dynamics via complex formation with lifetimes close to their rotation periods.

(R5) The fits were relatively insensitive and can account for reaction exoergicities between  $75 \pm 28$  and  $158 \pm 28 \text{ kJ mol}^{-1}$ . We also attempted to fit the laboratory data with lower reaction exoergicities down to  $33 \pm 10$  and  $22 \pm 10 \text{ kJ mol}^{-1}$ , i.e., the reaction energies associated with the formation of 1-phenyl-3-methylallene and 1-phenyl-butyne-2 as elucidated in our previous studies at collision energies as high as  $160 \text{ kJ mol}^{-1}$ . However, the laboratory data could not be fit with such low reaction energies.

First, let us consider the reaction energies. The experimentally determined reaction energies of  $75 \pm 28$  and  $158 \pm 28 \text{ kJ mol}^{-1}$  for the atomic hydrogen loss can account for the formation of methyl-substituted indenenes (**p5** and/or **p6**) ( $\Delta_{\text{R}}G = -166 \pm 10 \text{ kJ mol}^{-1}$ ;  $\Delta_{\text{R}}G = -153 \pm 10 \text{ kJ mol}^{-1}$ ) via intermediate **i6** and/or for the synthesis of **p4** ( $\Delta_{\text{R}}G = -72 \pm 10 \text{ kJ mol}^{-1}$ ) via unimolecular decomposition of **i2**. On the basis of the experimental energetics and a comparison with the theoretical data alone, we cannot determine which of these isomers is formed. However, the nondetection of the methyl group loss helps us to narrow down the remaining pathways further. Recall that if **i6** is formed, this intermediate should also decompose, besides atomic hydrogen loss forming methylindenenes (**p5** and/or **p6**), to indene (**p7**) at a level of 91% from our RRKM calculations. Therefore, the failed experimental detection of the methyl loss and hindered formation of indene (**p7**) indicates that **i6** is not formed predominantly. This can be understood easily due to the inherent barriers to isomerization; the initial collision complex **i1** either decomposes to **p1**, **p2**, and/or **p3**, or isomerizes via **i5** to **i2** with **i2** fragmenting to **p4**. Alternatively, the inherent barriers propose that the intermediate **i3**, if formed, rather eliminates atomic hydrogen or a methyl group yielding **p8**, **p9**, and/or **p10** respectively, or isomerizes via **i8** to **i2** with **i2** dissociating to **p4**.

Table 2. Product Branching Ratios Computed Using RRKM Rate Constants at Various Collision Energies

products	collision energy, kJ mol <sup>-1</sup>						
	10.46	20.92	31.38	41.84	52.00	62.76	156.00
	H Loss						
p1	0.00	0.00	0.00	0.01	0.01	0.03	0.46
p2	0.00	0.00	0.00	0.01	0.03	0.06	1.68
p4	87.44	87.06	86.69	86.23	85.72	84.97	66.56
p5	0.39	0.42	0.45	0.48	0.50	0.52	0.52
p6	0.52	0.58	0.64	0.70	0.75	0.80	0.92
p9	0.00	0.00	0.00	0.00	0.01	0.01	0.23
p10	0.00	0.00	0.00	0.01	0.01	0.03	0.84
	CH <sub>3</sub> Loss						
indene (p7)	11.63	11.88	12.05	12.20	12.24	12.26	9.00
p3	0.01	0.04	0.12	0.25	0.48	0.88	13.19
p8	0.00	0.02	0.05	0.12	0.24	0.44	6.60

Because 1,2-butadiene contains two carbon–carbon double bonds, three carbon atoms are involved in the  $\pi$ -system; these carbon atoms possess charges of  $-0.26$ ,  $0$ ,  $-0.20$ .<sup>24</sup> Therefore, the addition of phenyl to 1,2-butadiene would likely take place on the C1 and C3 carbon atoms, with the C1 carbon atom preferred due to the larger cone of acceptance as opposed to the C3 carbon atom. Note that the calculated barrier for C1 addition is only slightly lower than that for C3 addition. The nondetection of the methyl loss presents further consequences and narrows down the feasible reaction product(s), as **p3** and **p8** can be ruled out. Products **p1**, **p2**, **p9**, and **p10** can be eliminated (or, at least considered as less important) on the basis of the computed reaction energies of only  $13$ – $34$  kJ mol<sup>-1</sup>, which are too low to account for the experimental findings (Figure 3). Therefore, we state that the initial collision complexes **i1** and **i3** most likely isomerize to **i2** with the latter yielding **p4** via an atomic hydrogen loss. Further, the preferential formation of 2-phenyl-1,3-butadiene (**p4**) is also fully supported by our RRKM calculations. The computed branching ratio of **p4** is close to 86%, whereas the branching ratios of indene (**p7**) and methylindenes (**p5** and **p6**) are 12% and 1.2%, respectively, with the other products giving very minor contributions. The branching ratios do not vary significantly in the range of collision energies from 10 to 156 kJ mol<sup>-1</sup> (Table 2). The computed branching ratios do not change dramatically even at the collision energy of 156 kJ mol<sup>-1</sup> except an increase of the yield of the CH<sub>3</sub> loss products **p3** (**p8**) from **i1** (**i3**) to  $\sim 20\%$  in total, which, in comparison with the results of our previous experimental study,<sup>24</sup> points at a nonstatistical character of the reaction at the high collision energy.

To summarize, 2-phenyl-1,3-butadiene (**p4**) is suggested to be the major product formed in the reaction of phenyl with 1,2-butadiene under the single collision conditions at a collision energy of  $52 \pm 3$  kJ mol<sup>-1</sup>. Here, the reaction proceeds via indirect scattering dynamics through complex formation and is initiated by phenyl addition to the C1 or C3 carbon atoms of 1,2-butadiene leading to the initial collision complexes **i1** (**i3**). The latter isomerizes via a defacto phenyl group migration through bicyclic intermediate **i5** (**i8**) yielding **i2**, which eventually decomposes via a hydrogen atom loss from the methyl group of the 1,2-butadiene moiety leading to 2-phenyl-1,3-butadiene (**p4**). From the results of phenyl-*d*<sub>5</sub> reaction with 1,2-butadiene, this mechanism verifies that the emitted hydrogen atom originates from 1,2-butadiene, and not from the phenyl group.

It is also necessary to compare these findings with the results of the phenyl-1,2-butadiene reaction conducted at elevated

collision energies of up to 160 kJ mol<sup>-1</sup>. The previous study found that the thermodynamically less stable 1-phenyl-3-methylallene ( $\Delta_{\text{R}}G = -33 \pm 10$  kJ mol<sup>-1</sup>) and 1-phenyl-2-butyne ( $\Delta_{\text{R}}G = -24 \pm 10$  kJ mol<sup>-1</sup>) are the dominant reaction products formed via phenyl addition–hydrogen atom elimination pathways.<sup>24</sup> The authors proposed that the enhanced collision energy of up to 160 kJ mol<sup>-1</sup> defacto prohibits isomerization of the initial collision complex and rather favors a hydrogen atom elimination. However, considering the CM angular distributions, the reduced collision energy of only about 52 kJ mol<sup>-1</sup> at the present experiments increases the lifetimes of the initial collision complexes **i1**, **i2**, and/or **i3**, so that isomerization processes (via phenyl group migration) are feasible under the present experimental conditions. Therefore, we can conclude that the reaction products of the phenyl radical–1,2-butadiene system strongly depend on the collision energy, i.e., 1-phenyl-3-methylallene and 1-phenyl-2-butyne at higher collision energies and 2-phenyl-1,3-butadiene at lower collision energies. Recall that a similar trend has been observed previously in the reactions of the phenyl–methylacetylene/allene<sup>45</sup> and phenyl–1,3-butadiene reactions.<sup>23</sup> At elevated collision energies of up to 160 kJ mol<sup>-1</sup>, the reactions proceeded via simple phenyl radical addition–hydrogen atom elimination pathways leading to 1-phenylmethylacetylene (C<sub>6</sub>H<sub>5</sub>CCCH<sub>3</sub>) and 1-phenylallene (C<sub>6</sub>H<sub>5</sub>HCCCH<sub>2</sub>) for the phenyl–methylacetylene/allene system, and 1-phenyl-1,3-butadiene (C<sub>6</sub>H<sub>5</sub>CHCHCHCH<sub>2</sub>) for the phenyl–1,3-butadiene system, respectively. However, as the collision energy was lowered to about 45 kJ mol<sup>-1</sup>, the lifetimes of the initial collision complexes were found to increase, thus enabling successive isomerization steps via hydrogen migration and/or ring closures eventually, resulting in the formation of the aromatic indene<sup>22</sup> and 1,4-dihydronaphthalene<sup>26</sup> via atomic hydrogen loss, respectively.

## 5. CONCLUSION

We have explored the crossed molecular beam reactions of phenyl (C<sub>6</sub>H<sub>5</sub>; X<sup>2</sup>A<sub>1</sub>) and phenyl-*d*<sub>5</sub> (C<sub>6</sub>D<sub>5</sub>; X<sup>2</sup>A<sub>1</sub>) with 1,2-butadiene (C<sub>4</sub>H<sub>6</sub>; X<sup>1</sup>A') at low collision energies of  $52 \pm 3$  kJ mol<sup>-1</sup> under single collision conditions. We determined that 2-phenyl-1,3-butadiene (**p4**) likely presents the major product. The reaction of phenyl with 1,2-butadiene is initiated by adding the phenyl radical with its radical center to the  $\pi$  electron density at the C1/C3 carbon atom of 1,2-butadiene. The initial collision complexes isomerize via a defacto phenyl group migration from the C1/C3 to the C2 carbon atom of the 1,2-butadiene moiety. The resulting intermediate undergoes

unimolecular decomposition via hydrogen atom emission from the methyl group of the 1,2-butadiene moiety through a rather loose exit transition state leading to 2-phenyl-1,3-butadiene (**p4**). These results show that a change of collision energy can have a dramatic effect on the reaction products: 1-phenyl-3-methylallene and 1-phenyl-2-butyne at higher collision energies of up to  $160 \text{ kJ mol}^{-1}$ <sup>24</sup> and 2-phenyl-1,3-butadiene at lower collision energies of about  $52 \text{ kJ mol}^{-1}$ , as demonstrated in the present study. Further, the replacement of a hydrogen atom in allene by a methyl group was found to have a dramatic effect on the reactivity. Here, the methyl group cannot be considered as a spectator but is actively involved in the chemistry, as demonstrated by the decomposition of intermediate **i2** and hydrogen emission from the methyl group leading to 2-phenyl-1,3-butadiene (**p4**), which effectively minimizes the yield of the PAH products indene and methylindenes in the phenyl + 1,2-butadiene reaction.

## AUTHOR INFORMATION

### Corresponding Author

\*R. I. Kaiser: e-mail, ralfk@hawaii.edu; phone, 808-956-5731.

### Notes

The authors declare no competing financial interest.

## ACKNOWLEDGMENTS

We acknowledge the support from the US Department of Energy, Basic Energy Sciences, via grants DE-FG02-03ER15411 (Hawaii) and DE-FG02-04ER15570 (FIU).

## REFERENCES

- (1) Richter, H.; Howard, J. B. Formation of Polycyclic Aromatic Hydrocarbons and their Growth to Soot—A Review of Chemical Reaction Pathways. *Prog. Energy Combust. Sci.* **2000**, *26*, 565–608.
- (2) Duley, W. W. Polycyclic Aromatic Hydrocarbons, Carbon Nanoparticles and the Diffuse Interstellar Bands. *Faraday Discuss.* **2006**, *133*, 415–425.
- (3) Frenklach, M.; Feigelson, E. D. Formation of Polycyclic Aromatic-Hydrocarbons in Circumstellar Envelopes. *Astrophys. J.* **1989**, *341*, 372–384.
- (4) Hylland, K. J. Polycyclic Aromatic Hydrocarbon (PAH) Ecotoxicology in Marine Ecosystems. *J. Toxicol. Environ. Health A* **2006**, *69*, 109–123.
- (5) Tielens, A. G. G. M. Interstellar Polycyclic Aromatic Hydrocarbon Molecules. *Annu. Rev. Astron. Astrophys.* **2008**, *46*, 289–337.
- (6) Finlayson-Pitts, B. J.; Tropospheric, J. N. P. J. Air Pollution: Ozone, Airborne Toxics, Polycyclic Aromatic Hydrocarbons, and Particles. *Science* **1997**, *276*, 1045–1052.
- (7) Seinfeld, J. H.; Pankow, J. F. Organic Atmospheric Particulate Material. *Annu. Rev. Phys. Chem.* **2003**, *54*, 121–140.
- (8) Andres, R. J.; Boden, T. A.; Breon, F. M.; Ciais, P.; Davis, S.; Erickson, D.; Gregg, J. S.; Jacobson, A.; Marland, G.; Miller, J.; et al. A Synthesis of Carbon Dioxide Emissions from Fossil-fuel Combustion. *Biogeosciences* **2012**, *9*, 1845–1871.
- (9) Fu, P. P.; Beland, F. A.; Yang, S. K. Cyclopenta-Polycyclic Aromatic-Hydrocarbons - Potential Carcinogens and Mutagens. *Carcinogenesis* **1980**, *1*, 725–727.
- (10) Busby, W. F.; Stevens, E. K.; Kellenbach, E. R.; Cornelisse, J.; Lugtenburg, J. Dose-Response Relationships of the Tumorigenicity of Cyclopenta[Cd]Pyrene, Benzo[a]Pyrene and 6-Nitrochrysene in a Newborn Mouse Lung Adenoma Bioassay. *Carcinogenesis* **1988**, *9*, 741–746.
- (11) Durant, J. L.; Busby, W. F.; Lafleur, A. L.; Penman, B. W.; Crespi, C. L. Human Cell Mutagenicity of Oxygenated, Nitrated and Unsubstituted Polycyclic Aromatic Hydrocarbons Associated with Urban Aerosols. *Mutat. Res-Genet. Tox.* **1996**, *371*, 123–157.
- (12) Carl Sagan, B. N. K.; Thompson, W. R.; McDonald, G. D.; Wing, Michael R.; Bada, Jeffrey L.; Tuan Vo-Dinh, E. T. Arakawa Polycyclic Aromatic Hydrocarbons in the Atmospheres of Titan and Jupiter. *Astrophys. J.* **1993**, *414*, 399–405.
- (13) Schmitt-Kopplin, P.; Gabelica, Z.; Gougeon, R. D.; Fekete, A.; Kanawati, B.; Harir, M.; Gebefuegi, I.; Eckel, G.; Hertkorn, N. High Molecular Diversity of Extraterrestrial Organic Matter in Murchison Meteorite Revealed 40 Years after its Fall. *Proc. Natl. Acad. Sci. U. S. A* **2010**, *107*, 2763–2768.
- (14) Frenklach, M. Reaction Mechanism of Soot Formation in Flames. *Phys. Chem. Chem. Phys.* **2002**, *4*, 2028–2037.
- (15) Wang, H.; Frenklach, M. Calculations of Rate Coefficients for the Chemically Activated Reactions of Acetylene with Vinylic and Aromatic Radicals. *J. Phys. Chem.* **1994**, *98*, 11465–11489.
- (16) Kislov, V. V.; Islamova, N. I.; Kolker, A. M.; Lin, S. H.; Mebel, A. M. Hydrogen Abstraction Acetylene Addition and Diels-Alder Mechanisms of PAH Formation: A Detailed Study using First Principles Calculations. *J. Chem. Theory Comput.* **2005**, *1*, 908–924.
- (17) Tokmakov, I. V.; Park, J.; Lin, M. C. Experimental and Computational Studies of the Phenyl Radical Reaction with Propyne. *ChemPhysChem* **2005**, *6*, 2075–2085.
- (18) Yu, T.; Lin, M. C. Kinetics of the Phenyl Radical Reaction with Ethylene - an RRKM Theoretical-Analysis of Low and High-Temperature Data. *Combust. Flame* **1995**, *100*, 169–176.
- (19) Park, J.; Nam, G. J.; Tokmakov, I. V.; Lin, M. C. Experimental and Theoretical Studies of the Phenyl Radical Reaction with Propene. *J. Phys. Chem. A* **2006**, *110*, 8729–8735.
- (20) Park, J.; Burova, S.; Rodgers, A. S.; Lin, M. C. Experimental and Theoretical Studies of the  $\text{C}_6\text{H}_5+\text{C}_6\text{H}_6$  reaction. *J. Phys. Chem. A* **1999**, *103*, 9036–9041.
- (21) Parker, D. S. N.; Zhang, F. T.; Kim, Y. S.; Kaiser, R. I.; Landera, A.; Kislov, V. V.; Mebel, A. M.; Tielens, A. G. G. M. Low Temperature Formation of Naphthalene and its Role in the Synthesis of PAHs (Polycyclic Aromatic Hydrocarbons) in the Interstellar Medium. *Proc. Natl. Acad. Sci. U. S. A* **2012**, *109*, 53–58.
- (22) Parker, D. S. N.; Zhang, F. T.; Kaiser, R. I.; Kislov, V. V.; Mebel, A. M. Indene Formation under Single-Collision Conditions from the Reaction of Phenyl Radicals with Allene and Methylacetylene-A Crossed Molecular Beam and ab Initio Study. *Chem.—Asian J.* **2011**, *6*, 3035–3047.
- (23) Gu, X. B.; Zhang, F. T.; Kaiser, R. I. A Crossed Molecular Beam Study of the Phenyl Radical Reaction with 1,3-Butadiene and its Deuterated Isotopologues. *J. Phys. Chem. A* **2009**, *113*, 998–1006.
- (24) Gu, X. B.; Zhang, F. T.; Kaiser, R. I.; Kislov, V. V.; Mebel, A. M. Reaction Dynamics of the Phenyl Radical with 1,2-Butadiene. *Chem. Phys. Lett.* **2009**, *474*, 51–56.
- (25) Kaiser, R. I.; Zhang, F. T.; Gu, X. B.; Kislov, V. V.; Mebel, A. M. Reaction Dynamics of the Phenyl Radical ( $\text{C}_6\text{H}_5$ ) with 1-Butyne ( $\text{HCCC}_2\text{H}_5$ ) and 2-Butyne ( $\text{CH}_3\text{CCCH}_3$ ). *Chem. Phys. Lett.* **2009**, *481*, 46–53.
- (26) Kaiser, R. I.; Parker, D. S. N.; Zhang, F.; Landera, A.; Kislov, V. V.; Mebel, A. M. PAH Formation under Single Collision Conditions: Reaction of Phenyl Radical and 1,3-Butadiene to Form 1,4-Dihydronaphthalene. *J. Phys. Chem. A* **2012**, *116*, 4248–4258.
- (27) Golan, A.; Ahmed, M.; Mebel, A. M.; Kaiser, R. I. A VUV Photoionization Study on the Multichannel Reaction of Phenyl Radicals with 1,3-Butadiene under Combustion Relevant Conditions. *Phys. Chem. Chem. Phys.* **2013**, *15*, 341–347.
- (28) Kaiser, R. I.; Parker, D. S. N.; Goswami, M.; Zhang, F.; Kislov, V. V.; Mebel, A. M.; Aguilera-Iparraguirre, J.; Green, W. H. Crossed Beam Reaction of Phenyl and phenyl- $d_5$  Radicals with Propene and Deuterated Counterparts—Competing Atomic Hydrogen and Methyl Loss Pathways. *Phys. Chem. Chem. Phys.* **2012**, *14*, 720–729.
- (29) Guo, Y.; Gu, X. B.; Kawamura, E.; Kaiser, R. I. Design of a Modular and Versatile Interlock System for Ultrahigh Vacuum Machines: A Crossed Molecular Beam Setup as a Case Study. *Rev. Sci. Instrum.* **2006**, *77*, 034701.

(30) Gu, X. B.; Guo, Y.; Zhang, F. T.; Mebel, A. M.; Kaiser, R. I. Reaction Dynamics of Carbon-bearing Radicals in Circumstellar Envelopes of Carbon Stars. *Faraday Discuss.* **2006**, *133*, 245–275.

(31) Kaiser, R. I.; Maksyutenko, P.; Ennis, C.; Zhang, F. T.; Gu, X. B.; Krishtal, S. P.; Mebel, A. M.; Kostko, O.; Ahmed, M. Untangling the Chemical Evolution of Titan's Atmosphere and Surface from Homogeneous to Heterogeneous Chemistry. *Faraday Discuss.* **2010**, *147*, 429–478.

(32) Zhang, F. T.; Kim, S.; Kaiser, R. I. A Crossed Molecular Beams Study of the Reaction of the Ethynyl Radical ( $C_2H(X^2\Sigma^+)$ ) with Allene ( $H_2CCCH_2(X^1A_1)$ ). *Phys. Chem. Chem. Phys.* **2009**, *11*, 4707–4714.

(33) Bittner, J. D. *Ph.D. thesis*, Massachusetts Institute of Technology, Cambridge, MA 02139, U.S.A, 1981.

(34) Weiss, P. S. *Ph.D. thesis*, University of California at Berkeley, Berkeley, California 94720, U.S.A, 1986.

(35) Kaiser, R. I.; Le, T. N.; Nguyen, T. L.; Mebel, A. M.; Balucani, N.; Lee, Y. T.; Stahl, F.; Schleyer, P. V.; Schaefer, H. F. A Combined Crossed Molecular Beam and ab Initio Investigation of C(2) and C(3) Elementary Reactions with Unsaturated Hydrocarbons - Pathways to Hydrogen Deficient Hydrocarbon Radicals in Combustion Flames. *Faraday Discuss.* **2001**, *119*, 51–66.

(36) Maity, S.; Parker, D. S.; Dangi, B. B.; Kaiser, R. I.; Fau, S.; Perera, A.; Bartlett, R. J. A Crossed Molecular Beam and ab-Initio Investigation of the Reaction of Boron Monoxide (BO;  $X^2\Sigma^+$ ) with Methylacetylene ( $CH_3CCH$ ;  $X^1A_1$ ): Competing Atomic Hydrogen and Methyl Loss Pathways. *J. Phys. Chem. A* **2013**, *117*, 11794–11807.

(37) Kaiser, R. I.; Maity, S.; Dangi, B. B.; Su, Y.-S.; Sun, B.; Chang, A. H. A Crossed Molecular Beam and ab Initio Investigation of the Exclusive Methyl Loss Pathway in the Gas Phase Reaction of Boron Monoxide (BO;  $X^2\Sigma^+$ ) with Dimethylacetylene ( $CH_3CCCH_3$ ;  $X^1A_{1g}$ ). *Phys. Chem. Chem. Phys.* **2014**, *16*, 989–997.

(38) Levine, R. D. *Molecular Reaction Dynamics*; Cambridge University Press: Cambridge, U.K., 2005.

(39) Miller, W. B.; S. A. S, D. Herschbach Exchange Reactions of Alkali Atoms with Alkali Halides: a Collision Complex Mechanism. *Faraday Discuss.* **1967**, *44*, 108–122.

(40) Curtiss, L. A.; Raghavachari, K.; Redfern, P. C.; Baboul, A. G.; Pople, J. A. Gaussian-3 Theory Using Coupled Cluster Energies. *Chem. Phys. Lett.* **1999**, *314*, 101–107.

(41) Frisch, M. J.; Trucks, G. W.; Schlegel, H. B.; Scuseria, G. E.; Robb, M. A.; Cheeseman, J. R.; Montgomery, J. A.; Vreven, T.; Kudin, K. N.; Burant, J. C.; et al. *Gaussian 98*, Revision A.11; Gaussian, Inc.: Wallingford, CT, 2001.

(42) Werner, H.-J.; Knowles, P. J.; Amos, R. D.; Bernhardsson, A.; Berning, A.; Celani, P.; Cooper, D. L.; Deegan, M. J. O.; Dobbyn, A. J.; Eckert, F.; et al. *MOLPRO*, a Package of ab Initio Programs, Version 2002.1, 2002.

(43) Kislov, V. V.; Mebel, A. M. Ab Initio/RRKM-ME Study on the Mechanism and Kinetics of the Reaction of Phenyl Radical with 1,2-Butadiene. *J. Phys. Chem. A* **2010**, *114*, 7682–7692.

(44) Kislov, V. V.; Nguyen, T. L.; Mebel, A. M.; Lin, S. H.; Smith, S. C. Photodissociation of Benzene under Collision-free Conditions: An ab Initio/Rice-Ramsperger-Kassel-Marcus Study. *J. Chem. Phys.* **2004**, *120*, 7008–7017.

(45) Gu, X.; Zhang, F.; Guo, Y.; Kaiser, R. I. Reaction Dynamics of Phenyl Radicals ( $C_6H_5$ ,  $X^2A'$ ) with Methylacetylene ( $CH_3CCH$  ( $X^1A_1$ )), Allene ( $H_2CCCH_2$  ( $X^1A_1$ )), and their D4-Isotopomers. *J. Phys. Chem. A* **2007**, *111*, 11450–11459.